Running Head: Topographical memory and PCAI

A systematic study of topographical memory and posterior cerebral artery infarcts

Thomas Busigny (PhD) [1,2]
Bérengère Pagès [3]
Emmanuel J Barbeau (PhD) [2]
Clara Bled [2,3]
Emilie Montaut [3]
Nicolas Raposo (MD) [3,4,5]
Jean-François Albucher (MD) [3,4,5]
François Chollet (MD, PhD) [3,4,5]
& Jérémie Pariente (MD, PhD) [3,4,5]

[1] Institute of Psychology, Université Catholique de Louvain, Louvain-la-Neuve, Belgium
[2] Université de Toulouse UPS & Centre de Recherche Cerveau et Cognition (CNRS, Cerco, UMR 5549), Toulouse, France
[3] Service de Neurologie et Pôle Neurosciences, CHU de Toulouse, Toulouse, France
[4] Université de Toulouse, UPS, imagerie cérébrale et handicaps neurologiques UMR 825, CHU de Toulouse, Toulouse, France
[5] Inserm, imagerie cérébrale et handicaps neurologiques UMR 825, CHU de Toulouse, Toulouse, France

Manuscript word count: 2985
Abstract word count: 204
Title character count: 81
Number of references: 40
Number of tables & figures: 1 & 4
Supplemental data: 1 ('Busigny_Neurology_SupplementalData_Revised.pdf')

Dr Busigny[1,2] conducted the statistical analysis

Search terms: [6] Infarction; [38] Assessment of cognitive disorders; [120] MRI; [201] Memory; [203] Agnosia

Address all correspondence and reprint requests to:
Thomas Busigny
Cerco / Pavillon Baudot / CHU Purpan
Place du Dr Baylac
31059 Toulouse
E-Mail : busigny@cerco.ups-tlse.fr
Tel : +33 (0) 5 62 74 61 58
Fax : +33 (0) 5 62 74 61 17

Author contributions:

Dr. T. Busigny – study concept and design, analysis and interpretation
B. Pagès – study concept and design, acquisition of data
Dr E.J. Barbeau – study concept and design, critical revision of the manuscript for important intellectual content
C. Bled – acquisition of data
E. Montaut – acquisition of data
Dr N. Raposo – critical revision of the manuscript for important intellectual content
Dr J.-F. Albucher – critical revision of the manuscript for important intellectual content
Pr F. Chollet – critical revision of the manuscript for important intellectual content
Pr J. Pariente – study supervision

Financial disclosure statement:

Dr T. Busigny reports no disclosures
B. Pagès reports no disclosures
Dr E.J. Barbeau reports no disclosures
C. Bled reports no discolures
E Montaut reports no discolures
Dr N. Raposo reports no disclosures
Dr J.-F. Albucher received honoraria for medical scientific meetings from Bayer and Boehringer Ingelheim
Pr F. Chollet is a consultant for Institut de recherche Pierre Fabre, Pfizer and Boston Scientific
Pr J. Pariente serves as an editorial board member of Journal of Alzheimer's disease, and has received research grants from Avid pharmaceutics.

Abstract

Objective: To estimate the prevalence of topographical memory impairment following posterior cerebral artery infarcts (PCAI) and define its anatomical correlations.

Methods: We recruited 15 patients (mean duration of four months post infarct). We administered two sets of experimental tests to assess topographical memory: one set included five computerized tasks (CompT) and the other set consisted of one ecological topographical orientation test (EcolT) including four tasks (i.e., map drawing, pictures recognition and ordering, backward path). Fifteen healthy subjects participated as controls. Patients and controls underwent a volumetric T1 MRI brain scan. Brain lesions in patients were segmented, normalized and correlated with performance.

Results: Topographical memory impairments were evidenced in PCAI patients using both group and individual analyses (50%), with more severe outcomes in patients with PCAI in the right hemisphere. CompT and EcolT were highly correlated but the ecological test was more sensitive in revealed topographical memory impairments. Voxel-based lesion-symptom mapping demonstrated that two regions located in the cuneus and the calcarine sulcus correlated significantly with behavioral performance.

Conclusions: Topographical memory disorders following PCAI are reported in 50% of the patient's population. Our results demonstrate the importance of developing and using dedicated batteries of topographical memory tests, in particular real-life tests, to identify such deficits.

Keywords

Spatial memory, topographical orientation, posterior cerebral artery, ecological assessment, voxel-based lesion-symptom mapping

1. Introduction

Posterior Cerebral Artery Infarction (PCAI) accounts for 5-25% of ischemic strokes [1-3]. Visual field defect is the main symptom, followed by memory impairment, aphasia, dyslexia, hallucinations, hemineglect, visual agnosia and achromatopsia [4]. Topographical disorientation, defined as impaired orientation in one's familiar surroundings, is also sometimes reported [5-9], but has never been systematically studied. Such low interest in topographical memory after PCAI may seem paradoxical given that the topography of infarctions encompasses a wide network of brain areas involved in topographical orientation. Indeed, PCAI generally include the occipital, inferomedial temporal, and posterior parietal lobes [4;10], which overlaps with the brain regions (i.e. medial occipital, inferotemporal, posterior parahippocampal, posterior parietal and retrosplenial cortices) identified by neuropsychological and functional neuroimaging studies investigating topographical memory [9 ;11-15]. Considering the high frequency of PCAI, the lesions topography and the complaint of the patients, we conducted a systematic investigation of topographical memory in left and right PCAI patients. Our goal was to study the frequency of topographical memory impairment following PCAI and the relation between those defects and the localization of lesions.

2. Methods

Participants. From June 2010 to September 2013, consecutive patients with PCAI (n=21) from the neurology department of the university hospital of Toulouse Purpan were recruited. Six patients were excluded: one had a second stroke, one died during the assessment period, one was left-handed, and three stopped their participation during the protocol. In total, 15 PCAI patients participated in the entire study (7 left (L-PCAI), 8 right (R-PCAI)) (regarding the nature of the underlying vascular injury see details in Supplemental Table e-1). Patients (twelve males, all right-handed) were on average 51.6 year-old and their mean educational

level was 12.3 years (see details in Table 1). All of them completed a volumetric head MRI scan and underwent a comprehensive neuropsychological assessment with a mean delay of 124 days after the stroke. Fifteen healthy participants (nine males) participated in the study as control subjects (mean age: 52.3 years; mean educational level: 12.9 years). None of them had a history of neurological or vascular disease, head injury or alcohol abuse, or had cognitive complaints.

Standard protocol approvals, registrations, and patient consents. All patients and controls gave their written consent after detailed information. The study was approved by the institutional ethic committee (2-11-04; B110027-20).

Vision. All patients had a detailed ophthalmologic assessment including visual field (automated Humphrey field analyzer).

Topographical orientation complaint. Before the neuropsychological assessment, participants were asked whether they noticed any change in their topographical orientation since their stroke. If so they had to describe their complaint.

Neuropsychological assessment. First, all participants underwent a set of nine *background standardized tests* evaluating memory, language, praxis and visual functions (see Appendix e-1), including the bells tests (to assess hemineglect) and the Visual Object and Space Perception battery (VOSP) [16]. Then, they underwent a set of five *Computerized topographical memory tasks (CompT)***:** famous places recognition; new scenes memory; landmark recognition [17]; heading orientation [17]; route learning [18] (for details see Appendix e-1). Afterwards, participants were administered an *Ecological topographical orientation task (EcolT)* that took place in the precincts of the hospital ward (Figure 1). Participants walked with the examiner a specified route (length: 850m, decision-points: 30) after having been explicitly told to remember the route for a future test. After they reached the end of the route, participants were administered the map drawing task, the pictures

recognition task, the pictures ordering task, and required to walk back to the starting point of the pathway followed with the experimenter (i.e. backward path test) (for details see Appendix 1).

MRI brain scans. MRI scans were performed in all participants using a 3-T imager (Achieva; Philips, Best, The Netherlands), located in the Unit INSERM UMR825, Toulouse, France. Patients and controls underwent high-resolution anatomical images using a 3-D T1-weighted sequence (in-plane resolution 1×1mm, slice thickness 1mm, field of view 240×240mm, and 170 contiguous slices acquired in the sagittal plane, repetition time/echo time 8.1/3.7 ms, flip angle 8°).

Statistical analyses. The Mann–Whitney U was used for group comparisons between controls and patients and between L- and R-PCAI. Spearman's rank correlation coefficient was used for correlations. These analyses were conducted with SPSS 18.0 (IBM). In order to analyze individual profiles of L- and R-PCAI patients and due to the large variability of age among patients, each of them was compared to the four control subjects having the closest profile (in terms of gender and age, since these two variables are correlated with topographical orientation) [19]. To compare the results of single patients to these control subjects, a modified T-test for small samples of was used [20]. Performance was considered abnormal when the *p*-value was < 0.05 two-tailed. For the analysis of individual profiles, each test was converted to a modified z-score based on the mean, the standard deviation and the control sample size [20].

Analysis of brain imaging. Manual delineation of brain lesion was performed by two raters (TB & CB). The boundary of the lesion was manually delineated and filled on the individual native-space MRI image using MRIcron software (www.mricro.com) [21]. Then, the native original MR-images and the VOIs were nonlinearly transformed into MNI space (standard template of the Montreal Neurological Institute) using SPM 8 (Statistical Parameter

Mapping version 8 - Welcome Trust Centre for Neuroimaging, London, UK). Next, we calculated the percentage of overlap between each normalized VOI and Talairach regions according to the aal atlas provided by MRIcron (Anatomical Automatic Labelling) [22]. Finally, we conducted voxel-based lesion-symptom mapping (VLSM) [23], which allows to compare the performance of patients with and without a lesion of each voxel, with voxelwise statistics corrected for multiple comparisons over the whole brain (Brunner Munzel non-parametrical test; threshold: FDR $p<0.05$) (NPM package and MRIcron software, http://www.cabiatl.com/micro/).

3. Results

Demographics. Patients and controls were comparable in terms of age (U = 111; p = 0.97) and educational level (U = 83.5; p = 0.23). Similarly, there was no difference between left and right PCAI patients in terms of age (U = 20; p = 0.40) or educational level (U = 25.5; p = 0.78).

Vision. Visual field defects were found in 12 patients and were equally represented in left and right strokes: homonymous lateral hemianopia (L-PCAI: 3, R-PCAI: 3), homonymous bilateral hemianopia (L-PCAI: 1), homonymous superior quadrantanopia (L-PCAI: 1, R-PCAI: 1), homonymous inferior quadrantanopia (L-PCAI: 1, R-PCAI: 2) (see the average visual field defect in L- and R-PCAI in Supplemental Figure e-1). The level of visual field defect in L-PCAI and R-PCAI was equivalent (t_{150} = 1.35; p = 0.18).

Standardized neuropsychological tests. Patients obtained a globally normal neuropsychological profile (detailed in Supplemental Table e-2). No patient had sign of low-level perceptual impairment, hemineglect or simultagnosia (they all succeeded without difficulty the bells test and the spatial subtests of the VOSP). No significant difference between L- and R-PCAI was found.

Computerized topographical memory tasks (CompT). Results of controls and patients in the five tasks are summarized in Table 1. The only significant difference was found between controls and patients in the New scenes memory task ($U = 57.5$; $p < 0.05$).

Ecological topographical orientation task (EcolT). Results of controls and patients in the subtests are summarized in Table 1. The PCAI patients were significantly impaired in comparison to controls in the four subtests: recognition ($U = 47$; $p < 0.01$), ordering ($U = 36.5$; $p < 0.001$), backward path ($U = 43.5$; $p < 0.01$), map ($U = 55$; $p < 0.05$), and global score ($U = 33.5$; $p < 0.001$). Considered separately, L-PCAI patients obtained impaired scores in recognition ($U = 20$; $p < 0.05$), ordering ($U = 15$; $p < 0.01$) and backward path ($U = 9.5$; $p < 0.01$) subtests, and were globally impaired ($U = 13.5$; $p < 0.01$). R-PCAI patients obtained impaired scores in the recognition ($U = 27$; $p < 0.05$) and ordering ($U = 21.5$; $p < 0.05$) subtests and were globally impaired ($U = 22$; $p < 0.05$). No significant difference was found between L- and R-PCAI patients.

Computerized *vs* Ecological tasks. Computerized and ecological tasks were highly correlated, in the control group (*Rho* = 0.69; $p < 0.01$) as well as in the patients group (*Rho* = 0.80; $p < 0.001$) (Figure 2). Furthermore, patients performed better on the computerized than on the ecological task (*Wilcoxon* $Z = 3.41$; $p < 0.001$; Cohen's $d = 1.03$) while no difference was found in controls.

Individual results of the experimental tasks. When comparing each patient to four gender- and age-matched controls on computerized tasks, two L-PCAI (L1 & L5) and two R-PCAI (R2 & R4) were impaired. On the ecological task, four L-PCAI (L1, L2, L5 & L7) and four R-PCAI (R1, R2, R3 & R4) were impaired (Figure 3 and Supplemental Table e-3 for details). Most interestingly, the four most impaired patients are the four patients who complained about topographical disorientation (L2, R1, R2, R4). L2 reported that after her stroke she had to reflect more than before about familiar roads she wanted to use. R2 reported

having been lost on a very well known route. R1 complained about strong difficulties in remembering well known routes, in recognizing buildings and in getting oriented in new places. R4 was a taxi driver before his stroke, who could no longer drive his cab because he got lost in known places, had difficulties to plan routes and remember shortcuts. In our ecological task, L2 and R4 were impaired in the recognition subtest (respectively $p < 0.05$ and $p < 0.01$); R1, R2 and R4 were impaired in the ordering subtest (all ps < 0.01); L2, R1 and R4 were impaired in the backward pathway (all ps < 0.01); and R1, R2 and R4 were impaired in the map subtest (respectively $p < 0.05$, $p < 0.05$ and $p < 0.001$).

Lesion topography. The average lesion volume was identical in L-PCAI (10.3 mm3) and R-PCAI (6.9 mm3) patients ($U = 17$; $p = 0.23$) (see Supplemental Table e-4 for details). In R-PCAI patients, the main lesions were located in the lingual gyrus, calcarine sulcus and cuneus. In L-PCAI, the main lesions were located in lingual gyrus and calcarine sulcus (see Figure 4A and Supplemental Table e-5).

Anatomical-clinical correlations. No correlation was significant between anatomical data and behavioral results in computerized tasks, neither for L-, nor R-PCAI patients. Moreover, no correlation was significant between anatomical data and behavioral results in the ecological task in L-PCAI patients. However, we found significant correlations between anatomical data and the ecological task in R-PCAI patients: the global score of R-PCAI patients correlated with volume size ($Rho = -0.88$; $p < 0.01$), percentage of damage to the cuneus ($Rho = -0.73$; $p < 0.05$), and percentage of damage to the calcarine sulcus ($Rho = -0.76$; $p < 0.05$). These results were corroborated by Voxel-based lesion-symptom mapping (VLSM), comparing the performance of R-PCA patients with and without a lesion in each voxel, with voxelwise Z statistics corrected for multiple comparisons over the whole brain (threshold: FDR $p < 0.05$). Significant regions of correlation were located in the right cuneus

(923 voxels, 8%) and the right calcarine sulcus (352 voxels, 2.2%) (Figure 4B). No significant cluster was found in L-PCAI patients.

4. General Discussion

Our first goal was to determine whether PCAI may result in topographical memory deficits. Our results demonstrate that L-PCAI and R-PCAI indeed present impairments of spatial memory as groups. Analysis of individual profiles indicated that 8/15 patients presented impaired spatial memory. Thus, topographical memory deficit is a quite common consequence of PCAI. Interestingly however, such impairment was observed more easily on our ecological test of spatial memory than on our computerized tests. This suggests that topographical memory impairments may have been underestimated if only paper-and-pencil or computerized tests are used.

Group analyses demonstrated that both L-PCA and R-PCA presented topographical disorientation. However, after a careful look at individual profiles, and taking into account the age and gender of each patient, we demonstrate that R-PCAI patients were more severely affected than L-PCAI patients. This difference between left and right PCAI patients cannot be explained by other variables such as age, gender, educational level, visual field defect or general neuropsychological profile, since L- and R-PCAI patients were strictly equivalent on those variables.

The right hemisphere has long been considered as more specialized for the perceptual and cognitive analysis of space [24-26]. Recently, patients with vascular accident in the territory of the right middle cerebral artery performed worse than left-damaged patients and controls in a walking spatial span test [27]. In another ecological map-following task, right cerebrovascular brain-damaged patients performed worse than controls and left brain-damaged patients [28]. Together with these previous findings, our results demonstrated that

while both hemispheres seem involved in spatial memory, the posterior regions of the right hemisphere are particularly crucial in subserving spatial memory mechanisms.

Furthermore, we showed that the most impaired patients were those who complained about topographical orientation difficulties, demonstrating the link between subjective complaint and behavioral results in our tasks. Interestingly however, only four of the eight patients with impaired performance explicitly complained. Anosognosia of visual perception defects is frequent in PCAI patients, particularly when lesions encompass the lingual gyrus and the cuneus [29]. It would explain why 50% of the impaired patients failed to recognize consciously their topographical disorientation. Alternatively, the four less impaired patients could also have not noticed their deficits because these were too subtle to be noticed in real-life routine navigation.

Our results demonstrated that our ecological topographical orientation task was much more sensitive than the computerized tasks. Indeed, while patients and controls globally obtained the same performance in the computerized tasks, patients were significantly impaired at all the subtests of the ecological task. This difference cannot be explained by a difference in difficulty, since CompT and EcolT were performed equally well by controls. These results are in line with previous studies that demonstrated the higher validity of ecological tests in wayfinding assessment [30-31]. This discrepancy between classical or computerized tasks and ecological assessment could be explained by the fact that route learning in the real world depends on strategies in selecting perspectives and attending to landmarks in the distance that are missing in paper-and-pencil or using standard screens. These results support the use of ecological tasks as predictors of wayfinding skills and of real world functioning in PCAI.

The anatomical regions correlating with the behavioral performance were located in the cuneus and calcarine sulcus of the right hemisphere. This appears in line with a set of studies

which demonstrated that the activity of the cuneus specifically increases in tasks of wayfinding [32], familiar places recognition [33] and when subjects use a strategy based on spatial-associative representations for retrieval of objects location [34]. A recent study also found that the grey matter volume of the cuneus correlated with performance in a virtual water maze task [35]. Second, another set of study found that the right calcarine sulcus is involved in learning in navigational space [36-38]. The calcarine sulcus is also sometimes considered as a part of what was called the "retrospenial complex" [33] that is defined as a functional region including the anatomically defined retrosplenial cortex (Brodmann's areas 29 and 30), the posterior cingulate (area 23) and the anterior calcarine region. We indeed found lesions in the retrosplenial cortex as well as in the retrosplenial complex in our topographically disoriented patients (see Supplemental Table e-5). However, the VLSM results demonstrated that the region correlating significantly with the deficits was more posterior, in Brodmann's area 18, at the level of the cuneus and the calcarine sulcus.

Finally, it was suggested that visuospatial processing is subtended by the occipital-parietal circuit (also called dorsal stream) and three parietal pathways emerging from the dorsal stream: a parieto-prefrontal pathway (supporting spatial working memory), a parieto-premotor pathway (supporting visually guided actions), and a parieto-medial temporal pathway, which links the parietal lobe to the parahippocampal gyrus and the medial temporal lobe (supporting landmarks processing and spatial navigation) [39]. The latter pathway is connected to the occipital-parietal network via the angular gyrus. The angular gyrus shows strong functional connectivity with the precuneus and area V6 that are strongly connected with early visual areas in the region of the calcarine sulcus and the cuneus (see Fig.3 in [39]). Our patients who performed poorly in the ecological topographical orientation task might have a lesion that interrupts the occipito-parietal pathway and disconnects the parieto-medial temporal pathway. This could explain the specific navigational impairments in our R-PCAI patients with lesions

of the cuneus or the calcarine sulcus that are located on the occipito-parietal pathway. As a result, these patients would present impairment in landmark recognition and navigation because of a disconnection of the parieto-medial temporal pathway.

Anterograde topographical disorientation was previously associated with medial inferior occipital and medial occipitotemporal lesions, especially in the posterior parahippocampal gyrus [8-9;13]. In a recent study on cerebrovascular brain-damaged patients, significant associations were evidenced between lesioned voxels and spatial errors in the right putanem, superior longitudinal fasciculus and superior corona radiata [29]. In another study on PCAI patients, an overlap of lesions was found in the fusiform and parahippocampal gyrus in patients with impairment in house pictures memory [40]. Overall thus, considering our results together with these previous findings, spatial cognition relies on a posterior network of brain areas, mostly right lateralized, that are likely often damaged in PCAI.

We conducted a systematic investigation of topographical memory in left and right PCAI patients. Patients were recruited after a first and unique stroke, they all were at a chronic stage, on average four months post-infarct, and they underwent an extensive battery of behavioural, computerized and ecological tests. This study allowed us to demonstrate that topographical memory impairment is a frequent trait following PCAI, provided that sufficiently sensitive tests are used and considering the fact that patients often fail to recognize consciously their topographical disorientation. These results should encourage the systematic assessment of topographical memory with dedicated tests after PCAI.

Acknowledgments

Thank you to Aiden Arnold, Ford Burles and Giuseppe Iaria for sharing their tasks of landmark recognition and heading orientation. Many thanks to Laure Saint-Aubert and Federico Nemmi for their priceless help in brain imaging analysis. We also thank Marion Sarrail and Aude Deramond for testing patients, Ephraïm Partouche for his help with brain lesions delineation, Gwenaël Bourcier for the drawing in Figure 1, as well as Nadine Betbeder for her investment in creating the computerized spatial memory tasks. We thank Federico Nemmi and Giuseppe Iaria for their comments on a previous version of the manuscript and two anonymous reviewers for their helpful remarks. Finally, our gratitude goes to Nathalie Vayssière, Hélène Gros, Lucette Foltier and Jean-Pierre Désirat of the IRM technical platform (INSERM UMR825) for their priceless assistance. Thomas Busigny was supported by the Belgian National Fund for Scientific Research (FRS-FNRS).

References

[1] Yamamoto Y, Georgiadis AL, Chang HM, Caplan LR. Posterior cerebral artery territory infarcts in the New England Medical Center Posterior Circulation Registry. Arch Neurol 1999; 56:824-832.

[2] Brandt T, Steinke W, Thie A, Pessin MS, Caplan LR. Posterior cerebral artery territory infarcts: clinical features, infarct topography, causes and outcome. Multicenter results and a review of the literature. Cerebrovasc Dis 2000; 10:170-182.

[3] Arboix A, Arbe G, Garcia-Eroles L, Oliveres M, Parra O, Massons J. Infarctions in the vascular territory of the posterior cerebral artery: clinical features in 232 patients. BMC Research Notes 2011; 4:329.

[4] Cals N, Devuyst G, Asfar N, Karapanayiotides T, Bogousslavsky J. Pure superficial posterior cerebral artery territory infarction in The Lausanne Stroke Registry. J Neurol 2002; 249:855-861.

[5] Kraft A, Grimsen C, Kehrer S, et al. Neurological and neuropsychological characteristics of occiptal, occipito-temporal and occipito-parietal infarction. Cortex Epub 2012 Oct 27.

[6] Habib M & Sirigu A. Pure topographical disorientation: A definition and an anatomical basis. Cortex 1987; 23:73-85.

[7] Milandre L, Brosset C, Botti G, Khalil R. [A study of 82 cerebral infarctions in the area of posterior cerebral arteries]. Rev Neurol 1994; 150:133-141.

[8] Barrash J. A historical review of topographical disorientation and its neuroanatomical correlates. J Clin Exp Neuropsychol 1998; 20:807-827.

[9] Aguirre GK, D'Esposito M. Topographic disorientation: A synthesis and taxonomy. Brain 1999; 122:1613-1628.

[10] Park KC, Yoon SS, Rhee HY. Executive dysfunction associated with stroke in the posterior cerebral artery territory. J Clin Neurosci 2011; 18:203-208.

[11] Epstein RA, Kanwisher N. Acortical representation of the local visual environment. Nature 1998; 392:598-601.

[12] Aguirre GK, Zarahn E, D'Esposito M. Neural components of topographical representation. Proc Natl Acad Sci 1998; 95:839-846.

[13] Barrash J, Damasio H, Adolphs R, Tranel D. The neuroanatomical correlates of route learning impairment. Neuropsychologia 2000; 38:820-836.

[14] Epstein RA. Parahippocampal and retrosplenial contributions to human spatial navigation. Trends Cogn Sci 2008; 12:388-396.

[15] Vann SD, Aggleton JP, Maguire EA. What does the retrosplenial cortex do? Nat Rev Neurosci 2009; 10:792-802.

[16] Warrington EK, James M. The visual object and space perception battery. Bury St Edmunds: Thames Valley Test Company; 1985.

[17] Arnold AE, Burles F, Krivoruchko T, Liu I, Rey CD, Levy RM, Iaria G. Cognitive mapping in humans and its relationship to other orientation skills. Exp Brain Res 2013; 224:359-372.

[18] Barbeau EJ, Didic M, Felician O, Tramoni E, Guedj E, Ceccaldi M, Poncet M. Pure progressive amnesia: An atypical amnestic syndrome? Cogn Neuropsychol 2006; 23:1230-1247.

[19] Liu I, Levy, RM, Barton, JJS, Iaria G. Age and gender differences in various topographical orientation strategies. Brain Res 2011; 1410:112-119.

[20] Crawford JR, Howell DC. Comparing an individual's test score against norms derived from small samples. The Clinical Neuropsychologist 1998; 12:482-486.
[21] Rorden C, Karnath H-O, Bonilha L. Improving lesion-symptom mapping. J Cogn Neurosci 2007; 19:1081–1088.
[22] Tzourio-Mazoyer N, Landeau B, Papathanassiou D, Crivello F, Etard O, Delcroix N, Mazoyer B, Joliot M. Automated anatomical labeling of activations in SPM using a macroscopic anatomical parcellation of the MNI MRI single-subject brain. Neuroimage 2002; 15: 273-289.
[23] Bates E, Wilson SM, Saygin AP, Dick F, Sereno MI, Knight RT, Dronkers NF. Voxel-based lesion-symptom mapping. Nat Neurosci 2003; 6:448-450.
[24] Newcombe F, Russel WR. Dissociated visual perceptual and spatial deficits in focal lesions of the right hemisphere. J Neurol Neurosurg Psychiat 1969; 32;73-81.
[25] Ratcliff G, Newcombe F. Spatial orientation in man: effects of left, right, and bilateral posterior cerebral lesions. J Neurol Neurosurg Psychiat 1973; 36;448-454.
[26] De Renzi E, Faglioni P, Previdi P. Spatial memory and hemispheric locus of lesion. Cortex 1977; 13:424-433.
[27] Piccardi L, Iaria G, Bianchini F, Zompanti L, Guariglia C. Dissociated deficits of visuo-spatial memory in near space and navigational space: Evidence from brain-damaged patients and healthy older participants. Neuropsychol Dev Cogn B Aging Neuropsychol Cogn 2011; 18:362-384.
[28] Palermo L, Ranieri G, Boccia M, Piccardi L, Nemmi F, Guariglia C. Map-following skills in left and right brain-damaged patients with and without hemineglect. J Clin Exp Neuropsychol 2012; 34:1065-1079.
[29] Baier B, Geber C, Müller-Forell W, Müller N, Dieterich M, Karnath HO. Anosognosia for obvious visual field defect in stroke patients. Brain Struct Funct Epub 2014 Mar 21
[30] Naldone MJ, Stringer AY. Ecologic validity in neuropsychological assessment: Prediction of wayfinding. J Int Neuropsychol Soc 2001; 7:675-682.
[31] Monacelli AM, Cushman LA, Kavcic V, Duffy CJ. Spatial disorientation in Alzheimer's disease: the remembrance of things passed. Neurology 2003; 61:1491-1497.
[32] Hartley T, Maguire E, Spiers HJ, Burgess N. The well-worn route and the path less traveled: Distinct neural bases of route following and wayfinding in humans. Neuron 2003; 37:877-888.
[33] Epstein RA, Parker WE, Feller AM. Where am I now? Distinct roles for parahippocampal and retrosplenial cortices in place recognition. J Neurosci 2007; 27:6141-6149.
[34] de Rover M, Petersson KM, van der Werf SP, Cools AR, Berger HJ, Fernandez G. Neural correlates of strategic memory retrieval: Differentiating between spatial-associative and temporal-associative strategies. Hum Brain Mapp 2008; 29:1068-1079.
[35] Mueller SC, Merke DP, Leschek EW, Fromm S, Grillon C, Cornwell BR, Vanryzin C, Ernst M. Grey matter volume correlates with virtual water maze task performance in boys with androgen excess. Neuroscience 2011; 197:225-232.
[36] Iaria G, Chen J-K, Guariglia C, Ptito A, Petrides M. Retrosplenial and hippocampal brain regions in human navigation: complementary functional contributions to the formation and use of cognitive maps. Eur J Neurosci 2007; 25:890-899.
[37] Nemmi F, Boccia M, Piccardi L, Galati G, Guariglia C. Segregation of neural circuits involved in spatial learning in reaching and navigational space. Neuropsychologia 2013; 51:1561-1570.
[38] Nemmi F, Piras F, Péran P, Incoccia C, Sabatini U, Guariglia C. Landmark sequencing and route knowledge: An fMRI study. Cortex 2013; 49:507-519.

[39] Kravitz, DJ, Saleem KS, Baker CI, Mishkin M. A new neural framework for visuospatial processing. Nat Rev Neurosci 2011; 12:217-230.
[40] Martinaud O, Pouliquen D, Gérardin E, Loubeyre M, Hirsbein D, Hannequin D, Cohen L. Visual agnosia and posterior cerebral artery infarcts: An anatomical-clinical study. PLoS One 2012; 7:e30433.

Table 1

Top part of the table represents clinical and demographical data: gender, age, educational level, presence of visual field defect, presence of topographical memory complaint. Middle part of the table shows the results of patients and controls in the Computerized topographical memory tasks (CompT). The global score represents the average of the percentage of correct responses in the five tasks. Bottom part of the table represents the results of patients and controls in the Ecological topographical orientation task (EcolT). The global score represents the average of the percentage of correct responses in the four subtests. RT: reaction time, ms: millisecond.
The column 'patients' provides the results of L-PCAI and R-PCAI together. Mean performance is provided with standard deviation in brackets. Asterisks represent the significant differences between controls *vs.* patients, controls *vs.* L-PCAI, and controls *vs.* R-PCAI (Mann-Whitney U test). (* $p<0.05$)

Clinical and demographic data

	Controls	Patients	L-PCAI (n=7)	R-PCAI (n=8)
Gender	6F/9M	3F/12M	1F/6M	2F/6M
Age	52.3 (13.1)	51.6 (19.5)	55.6 (17.9)	48.1 (21.4)
Educational level (years)	12.9 (2.7)	12.3 (3.1)	11.7 (2.4)	12.9 (3.8)
Visual field defect (n)	0	12	6	6
Topog. memory complaint (n)	0	4	1	3
Computerized topographical memory tasks (CompT)				
Tests	Controls	Patients	L-PCAI (n=7)	R-PCAI (n=8)
Famous monuments (%)	78.11 (11.97)	74.78 (10.14)	72.14 (11.33)	77.09 (9.08)
Famous monuments (RT ms)	3645 (2066)	4302 (2535)	5226 (2716)	3493 (2221)
New scenes (%)	83.65 (11.11)	**75.25** (8.93) *	76.19 (10.00)	74.43 (8.49)
New scenes (RT ms)	2579 (856)	2351 (1110)	2764 (965)	1990 (1160)
Landmarks (%)	96.67 (6.17)	90.00 (13.09)	84.29 (16.18)	95.00 (7.56)
Landmarks (RT ms)	4488 (1318)	6208 (2851)	6975 (3536)	5537 (2106)
Orientation (%)	88.67 (10.60)	85.71 (18.28)	80.00 (18.97)	90.00 (17.73)
Orientation (RT ms)	3464 (1465)	4072 (2054)	4456 (2851)	3783 (1343)
Route (%)	83.11 (15.91)	74.67 (22.14)	75.24 (16.20)	74.17 (27.47)
Route (RT sec)	479 (42)	505 (51)	497 (51)	510 (54)
GLOBAL SCORE	*85.90 (7.67)*	*79.77 (10.90)*	*77.06 (12.84)*	*82.14 (9.07)*
Ecological topographical orientation task (EcolT)				
Tests	Controls	Patients	L-PCAI (n=7)	R-PCAI (n=8)
Recognition (%)	83.56 (7.50)	**73.78** (9.75) *	**71.90** (10.86) *	**75.42** (9.07) *
Recognition (RT sec)	190 (68)	250 (126)	240 (101)	259 (151)
Ordering (%)	80.89 (13.54)	**63.11** (12.57) *	**60.95** (13.57) *	**65.00** (12.22) *
Ordering(RT sec)	215 (94)	223 (130)	180 (69)	261 (162)
Backward path (%)	96.89 (4.95)	**84.00** (14.10) *	**80.48** (13.11) *	87.08 (15.06)
Backward path (RT sec)	713 (136)	783 (153)	839 (186)	735 (108)
Forward path (RT sec)	689 (47)	724 (87)	735 (95)	714 (84)
Forward/Backward Ratio (%)	1.12 (6.99)	3.35 (7.84)	5.75 (7.80)	1.26 (7.75)
Map (%)	71.67 (21.63)	**48.89** (29.27) *	46.19 (31.47)	51.25 (29.16)
Map (RT sec)	218 (119)	292 (162)	245 (151)	333 (169)
GLOBAL SCORE	*83.28 (8.59)*	***67.44*** *(13.64)* *	***64.88*** *(13.68)* *	***69.69*** *(14.12)* *

Figure 1. Drawn-to-scale outline of the hospital representing the route learned in the EcolT task

The route consisted of 30 intersections (11 right, 9 straight and 10 left turns) along 850m over around 11min. Four tests were administered. Map: participants were asked to draw on a blank map the entire route. Recognition: participants had to decide whether photographs of scenes had been seen or not during the route learning phase (15 targets, 15 distractors). Ordering: participants had to decide amongst 15 pairs of two pictures which scene had been seen first. Backward path: after a delay of thirty minutes, participants were asked to walk the path backward until the starting point.

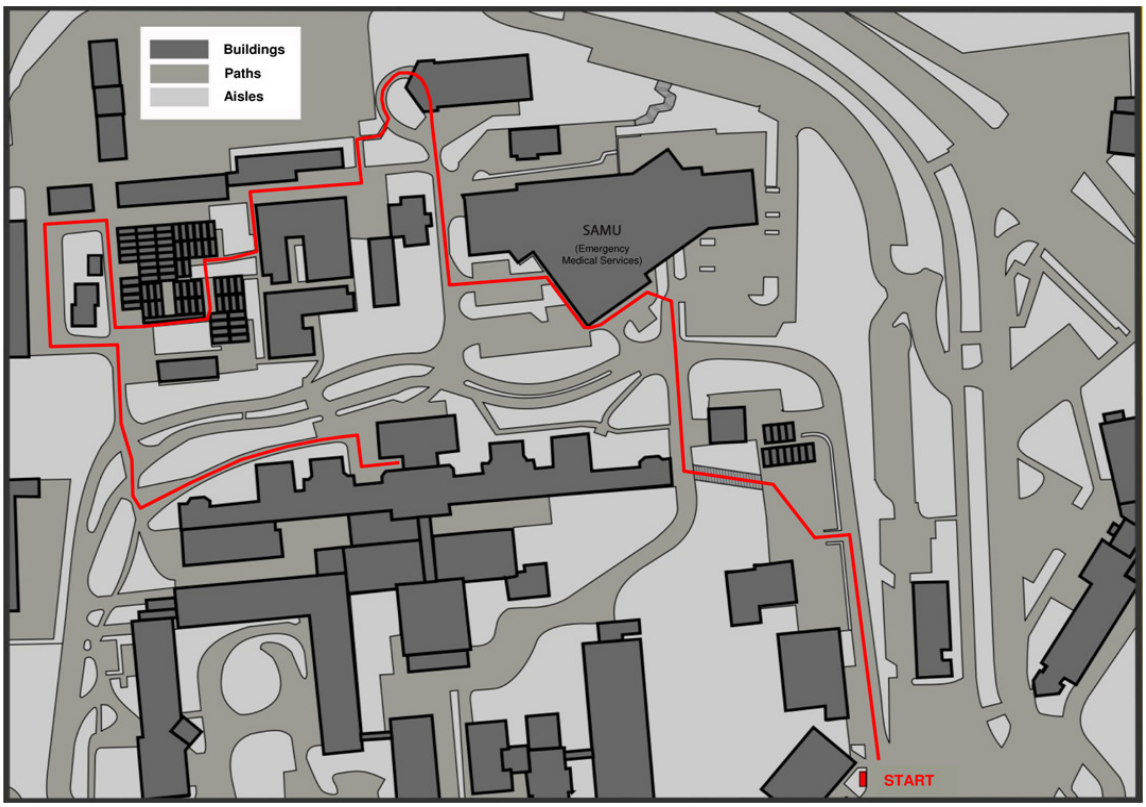

Figure 2. Correlation between results of computerized and ecological topographical tasks

Correlation between global scores from the Computerized topographical memory tasks (CompT) and the Ecological topographical orientation task (EcolT) for controls and patients.

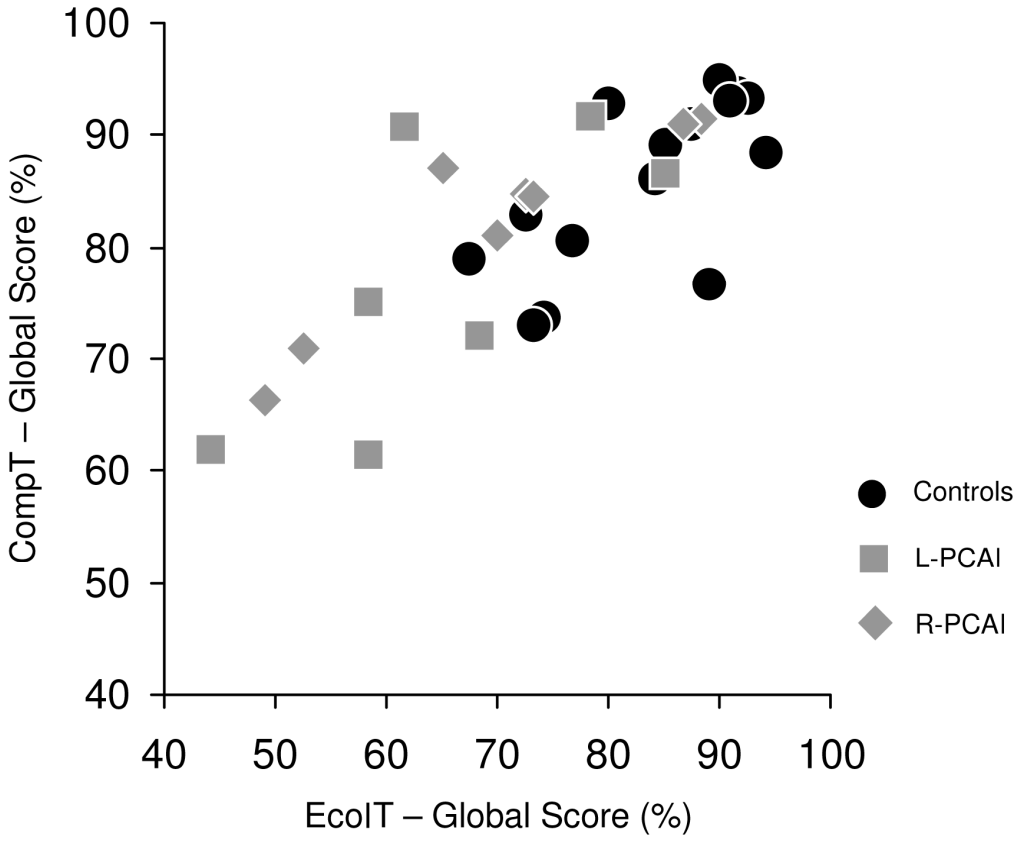

Figure 3. Individual profile of the PCAI patients

Individual profile of each of the PCAI patients compared to the best four matched control participants. Modified Z values were provided by the modified T-test of Crawford & Howell (1998) for single-case studies. In total, four patients were impaired in the CompT tasks (L1, L5, R2 & R4) and eight patients were impaired in the EcolT task (L1, L2, L5, L7, R1, R2, R3 & R4). All the patients impaired in CompT were also impaired in EcolT. Red rectangles indicate the four patients who complained about topographical disorientation.

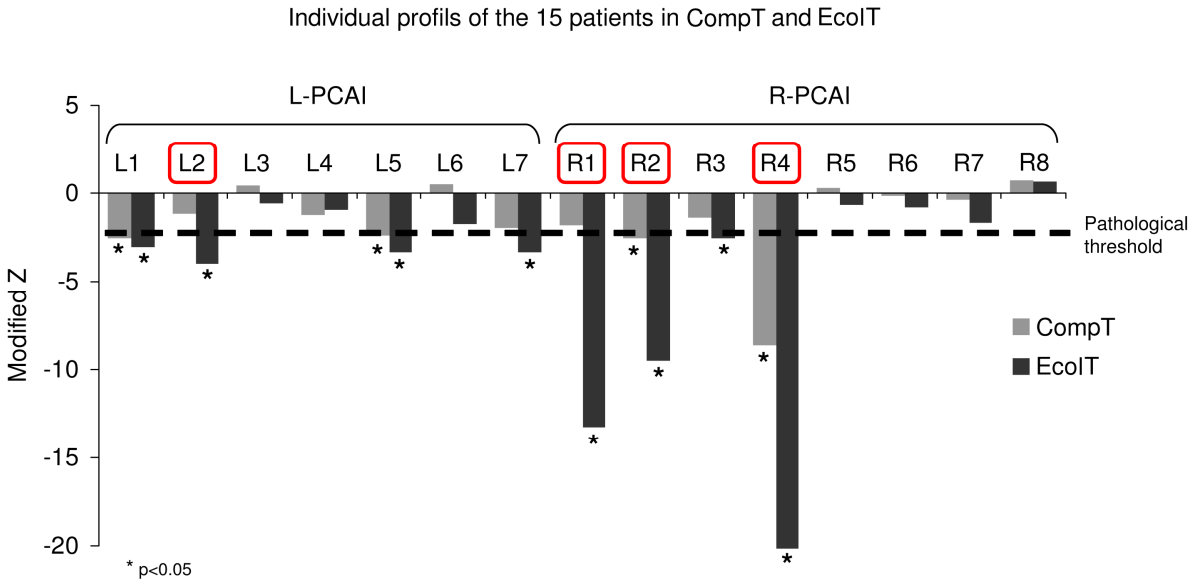

Figure 4. Overlap of lesion territories in L- and R-PCAI patients and VLSM results

(A) Overlap of lesion territories in left and right PCAI patients. The color scale from red to yellow represents the increasing number of damaged patients. Dark red represents regions were only one patient was damaged. Light yellow represents regions were five patients were damaged. In R-PCAI, the lesions were mainly located in lingual gyrus, calcarine sulcus and cuneus. In L-PCAI, the main lesions were located in lingual gyrus and calcarine sulcus. (B) Voxel-based lesion-symptom mapping (VLSM), comparing the performance of R-PCAI patients with and without a lesion in each voxel, with voxelwise Z statistics corrected for multiple comparisons over the whole brain (threshold: FDR $p < 0.05$). Significant regions are located in the cuneus (923 voxels, 8%) and the calcarine sulcus (352 voxels, 2.2%).

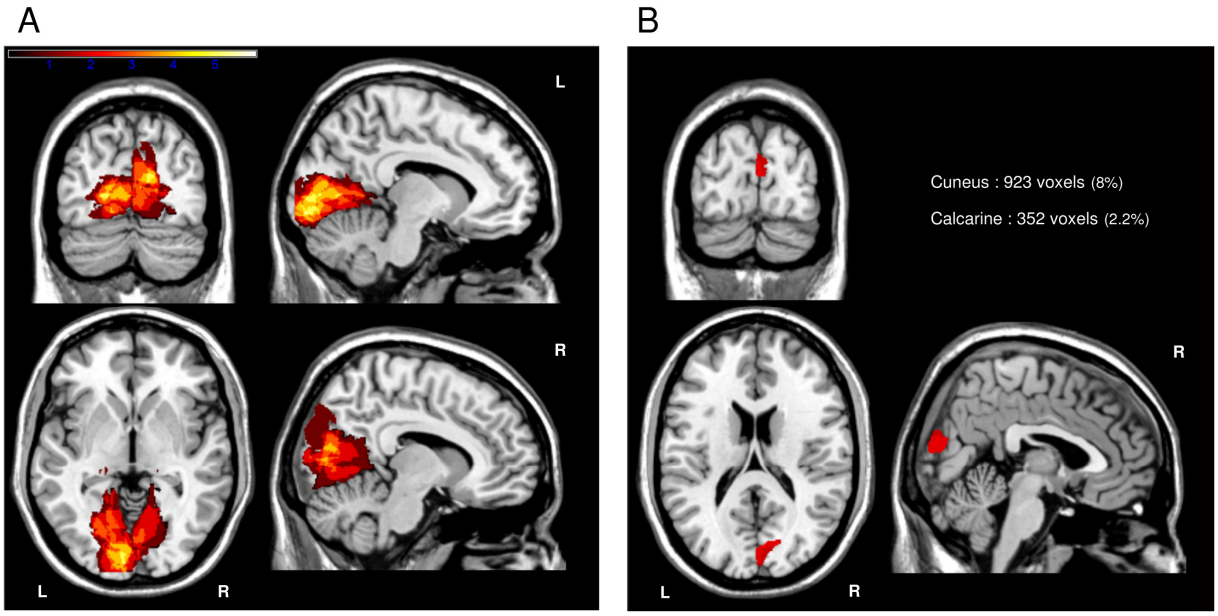

Appendix e-1

1. Standard neuropsychological tests.

All the participants underwent a set of nine background standardized tests evaluating memory, language, praxis and visual functions: (a) Rey figure copy and memory (Rey, 1958); (b) face memory subtest of WMS-III (Weschler, 2001); (c) verbal fluency (animal an first letter 'p'); (d) oral picture naming test (PicToul, Lepoutre, A., & Vieitez, A. (2010); (e) battery of gestural praxis; (f) forward and backward spatial span (Weschler, 2001); (g) the eight subtests of the Visual Object and Space Perception Battery (Warrington & James, 1985); (h) bells test for hemineglect (Gauthier et al., 1989); (i) Benton Face Recognition Test (BFRT, Benton et al., 1983).

2. Computerized topographical memory tasks (CompT).

The participants underwent a set of five computerized tasks assessing topographical memory**.** (a) ***Famous places recognition***. In this first task, participants saw a set of sixty pictures of monuments and sites. Half of them were famous (nationally, e.g., Avignon bridge, or internationally, e.,g., Big Ben) and the other half were unknown places. Each picture was presented one by one and participants had to decide if it represented a famous place or not by pressing a corresponding key. Number of correct responses and average response time for correct trials were recorded. (b) ***New scenes memory***. This experiment started with a set of thirty pictures of visual scenes to learn (representing landscapes and cityscapes). Each scene was presented one by one for 2 sec. Thirty minutes after the learning phase, participants saw a new set of forty-five pictures of scenes (fifteen seen in the learning phase and thirty new ones). They had to decide for each picture whether they saw it or not during the learning phase by pressing a corresponding key. Number of correct responses and average response time for correct trials were recorded. (c) ***Landmark recognition.*** This task published by Arnold and colleagues (2013) consisted in a virtual environment in which participants were

shown video clips of passive first-person perspective movement through a featureless environment in which unique landmarks were encountered along a set path. At the end of the video clip, participants were asked to identify these landmarks amongst four presented images displaying similar landmarks (e.g. identifying the correct bench across four different benches). Number of correct responses and average response time for correct trials were recorded. (d) ***Heading orientation.*** This second task published by Arnold and colleagues (2013) consisted in the same virtual environment than in the previous task. In each trial, participants were shown a 30-s video clip of passive first-person perspective movement in which three landmarks were encountered at intersections along a set path. One of the three landmarks encountered was shown at the end of each clip, and participants were asked to indicate whether a left or a right turn was taken at it. Number of correct responses and average response time for correct trials were recorded. (e) ***Route learning.*** This last task consisted in route learning in a virtual environment (see Barbeau et al., 2006). The itinerary was video-recorded from the front of a car driving through the suburb of a town unknown to all participants from the perspective of the driver. The video was shown on two consecutive occasions. The length of the itinerary was about 4 km, it lasted for 6 minutes and contained 15 decision points. Thirty minutes after the learning phase, the participants saw the video again. At each intersection, they had to decide whether the car had to turn right, turn left, or continue straight ahead. Number of correct responses and total response time were recorded. To obtain a total score representing the global performance in CompT, we calculated the average of the percentage of correct responses in the five tasks.

3. Ecological topographical orientation task (EcolT).

We devised a real-world navigational task in the precincts of the hospital ward (see Figure 1). Participants were taken by the examiner on a specified route and were instructed to attend to the route and the environment because they would later be asked to undergo testing related

to it. The route consisted of 30 intersections (11 right, 9 straight and 10 left turns) along 850 m over around 11 min. None of the participants was familiar with this area of the hospital. On completion of the route, four tests were administered. (a) ***Map***. First, the capacity to graphically represent survey knowledge of the route was assessed by a route-drawing task. A drawn-to-scale outline of the hospital (Figure 1) was provided together with only three indications: the starting point, the position of the Emergency Medical Services and the colours representing buildings, paths and aisles. Participants were asked to draw, as precisely as possible, the entire route until the end of the path (that was no represented on the map). Responses were considered correct when the line drawn was consistent with directions of the test route. Number of correct responses (max 30) and total response time were recorded. (b) ***Recognition***. To assess visual recognition of scenes from the route, thirty photographs were presented (fifteen from the participant's view of the test path and fifteen of other locations in the hospital). Pictures were presented one by one, and the participant had to decide for each photograph whether it was seen or not during route learning. Number of correct responses (max 30) and total response time were recorded. (c) ***Ordering***. In the next task, participants saw thirty new photographs of the test path. Each photograph represented a scene that was encountered during route learning. Pictures were presented in pairs, and participants had to decide which scene was seen first. Number of correct responses (max 15) and total response time were recorded. (d) ***Backward path***. After a delay of thirty minutes, participants were taken back at the end point of the route and were asked to walk the path backward until the starting point. They were instructed to follow the path as precisely as possible and did not get and cue from the examiner. In the case a participant took the wrong direction, the examiner stopped him after a couple of meters and brought him to the correct direction. Number of correct directions (max 30) and total response time were recorded. A ratio between forward route duration and backward route duration was calculated to take into account hesitations

and possible slowing down during the backward route (formula: (backward duration – forward duration) / (backward duration + forward duration)). Finally, to obtain a total score representing the global performance in EcolT, we calculated the average of the percentage of correct responses in the four subtests.

Supplemental table e-1

Nature of the underlying vascular injury in the 15 patients of the study (L = L-PCAI; R = R-PCAI).

	Nature of the injury
L1	Thrombotic
L2	Embolic
L3	Unknown
L4	Thrombotic
L5	Thrombotic
L6	Embolic
L7	Unknown
R1	Unknown
R2	Embolic
R3	Thrombotic
R4	Embolic
R5	Thrombotic
R6	Thrombotic
R7	Unknown
R8	Unknown

Supplemental table e-2

Results of patients (L = L-PCAI; R = R-PCAI) and controls in the standard neuropsychological tests. The column 'patients' provides the results of L-PCAI and R-PCAI together. Mean performance is provided with standard deviation in brackets. Asterisks represent the significant differences between controls *vs.* patients, controls *vs.* L-PCAI, and controls *vs.* R-PCAI (Mann-Whitney U test). (* $p<0.05$)

Tests	Controls	Patients	L-PCAI	R-PCAI
Rey Copy	34.80 (2.68)	33.93 (2.89)	33.14 (3.67)	34.63 (2.00)
Rey Memory	22.80 (5.62)	19.93 (5.58)	17.36 (5.65)	22.19 (4.74)
Face WMS-III immediate	37.40 (3.81)	35.00 (4.63)	34.57 (4.28)	35.38 (5.18)
Face WMS-III delayed	39.20 (3.95)	36.87 (5.37)	37.00 (5.94)	36.75 (5.23)
Verbal Fluency 'animal'	33.40 (8.80)	29.14 (8.24)	29.29 (10.95)	29.00 (5.20)
Verbal Fluency 'P'	23.67 (7.03)	**16.64** (4.55) *	17.86 (5.55)	**15.43** (3.26) *
Oral Picture Naming	19.64 (0.63)	19.40 (0.99)	19.29 (0.95)	19.50 (1.07)
Gestural Praxis	98.50 (2.79)	96.55 (5.10)	94.17 (6.31)	98.93 (1.85)
Forward Spatial Span	6.13 (0.74)	**5.20** (1.21) *	**5.14** (1.07) *	5.25 (1.39)
Backward Spatial Span	5.33 (0.72)	5.13 (1.46)	4.86 (1.77)	5.38 (1.19)
VOSP	93.76 (2.90)	91.43 (5.06)	90.00 (6.89)	92.86 (1.79)
Bells Test	34.13 (1.64)	33.80 (2.27)	33.00 (3.21)	34.50 (0.53)
Benton Face Recognition	48.93 (3.65)	**45.87** (3.46) *	45.88 (3.67)	**45.86** (3.52) *

Supplemental table e-3

Comparison of each patient to the four best matched controls in terms of gender and age on CompT an EcolT. T values and *p*-values were provided by the modified T-test of Crawford & Howell (1998) for single-case studies. (* p<0.05)

	CompT	EcolT
L1	**t_3 = 2.53 (p < 0.05) ***	**t_3 = 3.03 (p < 0.05) ***
L2	t_3 = 1.18 (p = 0.16)	**t_3 = 3.97 (p < 0.05) ***
L3	t_3 = 0.43 (p = 0.35)	t_3 = 0.56 (p = 0.31)
L4	t_3 = 1.22 (p = 0.16)	t_3 = 0.97 (p = 0.20)
L5	**t_3 = 2.42 (p < 0.05) ***	**t_3 = 3.33 (p < 0.05) ***
L6	t_3 = 0.48 (p = 0.33)	t_3 = 1.76 (p = 0.09)
L7	t_3 = 1.93 (p = 0.08)	**t_3 = 3.31 (p < 0.05) ***
R1	t_3 = 1.79 (p = 0.09)	**t_3 = 13.3 (p < 0.001) ***
R2	**t_3 = 2.50 (p < 0.05) ***	**t_3 = 9.53 (p < 0.01) ***
R3	t_3 = 1.35 (p = 0.14)	**t_3 = 2.52 (p < 0.05) ***
R4	**t_3 = 8.61 (p < 0.01) ***	**t_3 = 20.6 (p < 0.001) ***
R5	t_3 = 0.31 (p = 0.39)	t_3 = 0.63 (p = 0.29)
R6	t_3 = 0.16 (p = 0.44)	t_3 = 0.81 (p = 0.24)
R7	t_3 = 0.33 (p = 0.38)	t_3 = 1.66 (p = 0.10)
R8	t_3 = 0.72 (p = 0.26)	t_3 = 0.64 (p = 0.28)

Supplemental table e-4

Lesion volume (in mm^3) by patient (L = L-PCAI; R = R-PCAI).

	Lesion volume (mm^3)
L1	14280
L2	2412
L3	17445
L4	11123
L5	10376
L6	1996
L7	14349
Mean	**10283**
R1	9696
R2	9018
R3	8268
R4	20233
R5	3114
R6	3592
R7	237
R8	1061
Mean	**6902**

Supplemental table e-5

Percentage of lesion by anatomical region (L = L-PCAI; R = R-PCAI). The percentage represents the proportion of area that was damaged. The top part of the table represents the Talairach's areas. The bottom part of the table represents the Brodmann's areas (7: somatosensory association cortex; 17: primary visual cortex; 18: secondary visual cortex; 19: associative visual cortex; 20: inferior temporal gyrus; 23: ventral posterior cingulate; 27: piriform cortex; 29: retrosplenial cingulate; 30: cingulate; 37: fusiform gyrus).

	Lingual	Calcarine	Cuneus	Precuneus	Fusiform	Parahipp	Inf Occ	Mid Occ	Sup Occ	Thalamus
L1	26.4	30.8			0.9		7.7	2.9	4.5	
L2	12.2				0.7	1.8				
L3	38.3	46.7	4.3	0.6	0.5		1		3.2	
L4	45.1	11.1			2	1.1			2.1	
L5	5.7	19.3	2				10.8	8.1	14.9	
L6	6.8	2.2					4.1			
L7	23.6	41	0.8		4.1		0.6			14
R1	4.1	45.2	16.7	0.5						
R2	27.4	5.1			9	10.3				
R3		10	53.8						1.1	
R4	46.7	46.1	21.2	3.7	1.6	1.7				3.5
R5	0.5	17.6	1							
R6	2.6	18.4	0.7							
R7		1.2								
R8		5.9	1.6							
	Area 7	Area 17	Area 18	Area 19	Area 20	Area 23	Area 27	Area 29	Area 30	Area 37
L1		19.4	7.7	2.4					0.2	
L2		0.2	1.9	0.5			0.4		2.0	0.1
L3		24.7	9.4	2.5			1.8	0.4	1.1	
L4		10.7	6.2	2.1			1.3		3.6	0.6
L5		14.7	6.6	0.8						
L6		0.2	2.5							
L7		22.1	5.6	1.2			3.9		0.3	0.4
R1		16.4	4.1	0.3		0.5			0.2	
R2		5.8	3.1	1.5	0.1		2.9		3.9	2.5
R3	0.6	1.2	5.8	2.3						
R4		22.3	10.9	1.6		4.3	3.5	2.5	5.0	
R5		4.4	1.5	0.5						
R6		6.2	1.3	0.4						
R7		0.5								
R8		0.931	0.9	0.08						

Supplemental figure e-1

Representation of the average visual field defect in L-PCAI and R-PCAI (from 0: total visual defect to 32: perfect vision).